Stereoscopic slant contrast revisited

Frederick A. A. Kingdom McGill Vision Research, Department of Ophthalmology, Montréal General Hospital, Montréal, QC, Canada

Yoel Yakobi McGill Vision Research, Department of Ophthalmology, Montréal General Hospital, Montréal, QC, Canada

Xingao (Clara) Wang McGill Vision Research, Department of Ophthalmology, Montréal General Hospital, Montréal, QC, Canada

The perceived slant of a stereoscopic surface is altered by the presence of a surrounding surface, a phenomenon termed stereo slant contrast. Previous studies have shown that a slanted surround causes a fronto-parallel surface to appear slanted in the opposite direction, an instance of "bidirectional" contrast. A few studies have examined slant contrast using slanted as opposed to fronto-parallel test surfaces, and these also have shown slant contrast. Here, we use a matching method to examine slant contrast over a wide range of combinations of surround and test slants, one aim being to determine whether stereo slant contrast transfers across opposite directions of test and surround slant. We also examine the effect of the test on the perceived slant of the surround. Test slant contrast was found to be bidirectional in virtually all test–surround combinations and transferred across opposite test and surround slants, with little or no decline in magnitude as the test–surround slant difference approached the limit. There was a weak bidirectional effect of the test slant on the perceived slant of the surround. We consider how our results might be explained by four mechanisms: (a) normalization of stereo slant to vertical; (b) divisive normalization of stereo slant channels in a manner analogous to the tilt illusion; (c) interactions between center and surround disparity-gradient detectors; and (d) uncertainty in slant estimation. We conclude that the third of these (interactions between center and surround disparity-gradient detectors) is the most likely cause of stereo slant contrast.

Introduction

The perceived slant of a random-dot stereoscopic surface is altered by the presence of a surrounding slanted surface, a phenomenon termed stereo slant contrast (Gillam & Pianta, 2005; Goutcher & Wilcox, 2021; Graham & Rogers, 1982; Poom, Olsson, & Börjesson 2007; Rogers, Cagenello, & Rogers, 1988; van der Kooij & te Pas, 2009a; van der Kooij & te Pas, 2009b; van Ee, Banks, & Backus, 1999; Wardle & Gillam, 2016; reviewed in Howard & Rogers, 2002). Here, we use the term "slant" to characterize a planar surface oriented around the horizontal axis (as, for example, in Oluk, Bonnen, Burge, Cormack, & Giesler, 2022)—in other words, an inclination (although note that others have defined "slant" as a surface oriented around a vertical axis and hence distinct from inclination; e.g., Howard & Rogers, 2002). Stereo slant contrast is "bidirectional" in that the perceived slant of the test surface is invariably shifted away from that of the surround surface (see Figure 1). To our knowledge, most previous studies have tested stereo slant contrast using fronto-parallel surfaces—in other words, "vertical" test surfaces as in Figure 1—and only a couple of studies have measured stereo slant contrast with slanted test surfaces (van der Kooij & te Pas, 2009a; van der Kooij & te Pas, 2009b). Moreover, we are unaware of any studies that have measured stereo slant contrast using tests and surrounds whose slant angles are of opposite sign (e.g., when viewed from the side, the test is slanted like / and the surround like \ or vice versa).

In this study, we measured the stereo slant contrast of a central test stimulus across a wide range of test and surround slants. We also measured the effect of the central test on the perceived stereo slant of the surround. The results have enabled us to obtain a more complete picture of the properties of stereo slant contrast and hence to help constrain the possible mechanisms for stereo slant contrast.

Citation: Kingdom, F. A. A., Yakobi, Y., & Wang, X. (Clara) (2024). Stereoscopic slant contrast revisited. *Journal of Vision*, *24*(4):24, 1–14, https://doi.org/10.1167/jov.24.4.24.

https://doi.org/10.1167/jov.24.4.24 Received September 4, 2023; published April 29, 2024 ISSN 1534-7362

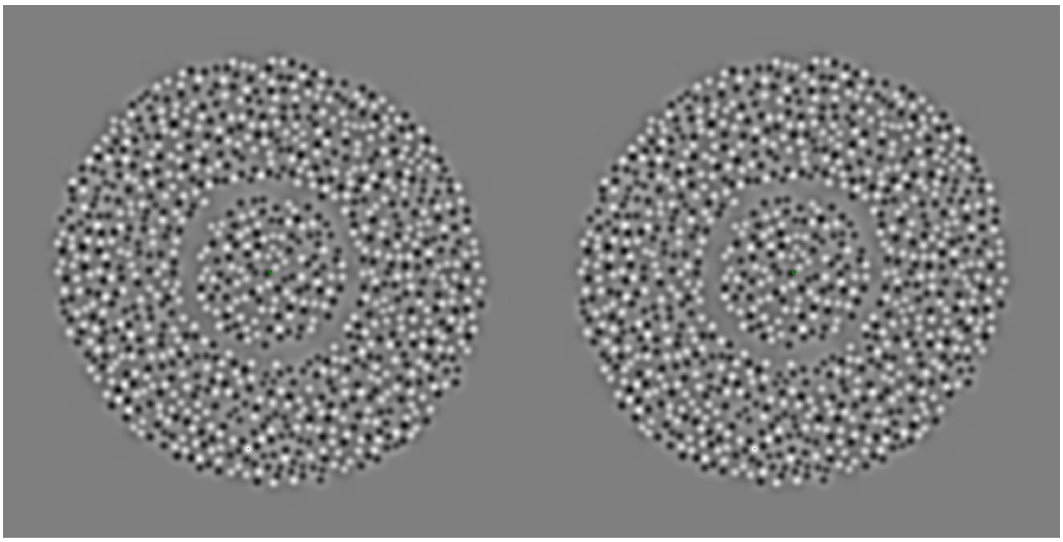

Figure 1. Example stimulus stereo pair. The surround has a slant of –35° when cross-fused and the test is fronto-parallel, or 0°. Free fusion should reveal a test surface that appears lightly slanted in the opposite direction to that of the surround.

Methods

Observers

Three authors and an undergraduate volunteer participated as observers. All observers had normal or corrected-to-normal visual acuity. Observer 1 had only superficial knowledge and observers 2 and 4 had no knowledge about the purpose of the experiment when tested. Observer 4 completed only a subset of the range of conditions. All experiments were conducted in accordance with the tenets of the Declaration of Helsinki and the Research Institute of the McGill University Health Centre Ethics Board.

Stimulus display

All experiments were conducted using a Dell Precision T1650 PC (Dell Technologies, Round Rock, TX) with a ViSaGe graphics card (Cambridge Research Systems, Kent, UK). The stereo pairs were displayed on either side of a gamma-corrected Sony Trinitron Multiscan F500 flat-screen CRT monitor (Sony Corporation, Tokyo, Japan). Stimulus generation and control employed custom software written in C/C++ with embedded ViSaGe graphics routines. Participants viewed the stereo pairs through a custom-built eight-mirror stereoscope with an aperture of 10° × 15° and a viewing distance along the light path of 105 cm.

Stimuli

An example test-plus-surround stereo pair is shown in Figure 1. All stimuli were circular. The test and match stimuli were both 3.0° in diameter. The surround had a diameter of 8.5° and was separated from the test by a 0.35° gap, an amount that pilot work suggested should help observers distinguish the center from the surround. Due to the relative lateral displacement of the test and surround micropatterns necessary to achieve stereoscopic depth, the width of the gap differed between the two monocular images by varying amounts around its circumference. However, in the cyclopean view, the gap width appeared uniform, and we see no reason why the small monocular differences in gap width would affect our results.

Each test-and-surround combination was composed of 1000 two-dimensional Laplacian of Gaussian (LoG) micropatterns with a standard deviation (*SD*) of 0.08°. The LoG micropatterns were positioned as follows: On each trial, 1000 Gaussian functions, each with unit peak amplitude, were randomly positioned within a virtual window the size of the stimulus but with the constraint that no two Gaussians overlapped if their maximum summed amplitude exceeded 1.25. The coordinate positions of the resulting set of Gaussians defined the positions of the LoGs in the stimulus. The disparity of each LoG was achieved by selecting it from one of 200 templates, with the LoG in each template horizontally offset from the template center with subpixel accuracy by an amount ranging from −0.5° to +0.5°, resulting in a disparity resolution of 0.005°. The use of precomputed templates minimized the time required to generate the stimuli afresh on each trial. Template pairs with opposite but equal-in-magnitude disparities were then positioned into their preallocated locations in the two stereo halves, but with the contrast polarity of each pair randomized. The contrast of the stimulus as a whole was scaled

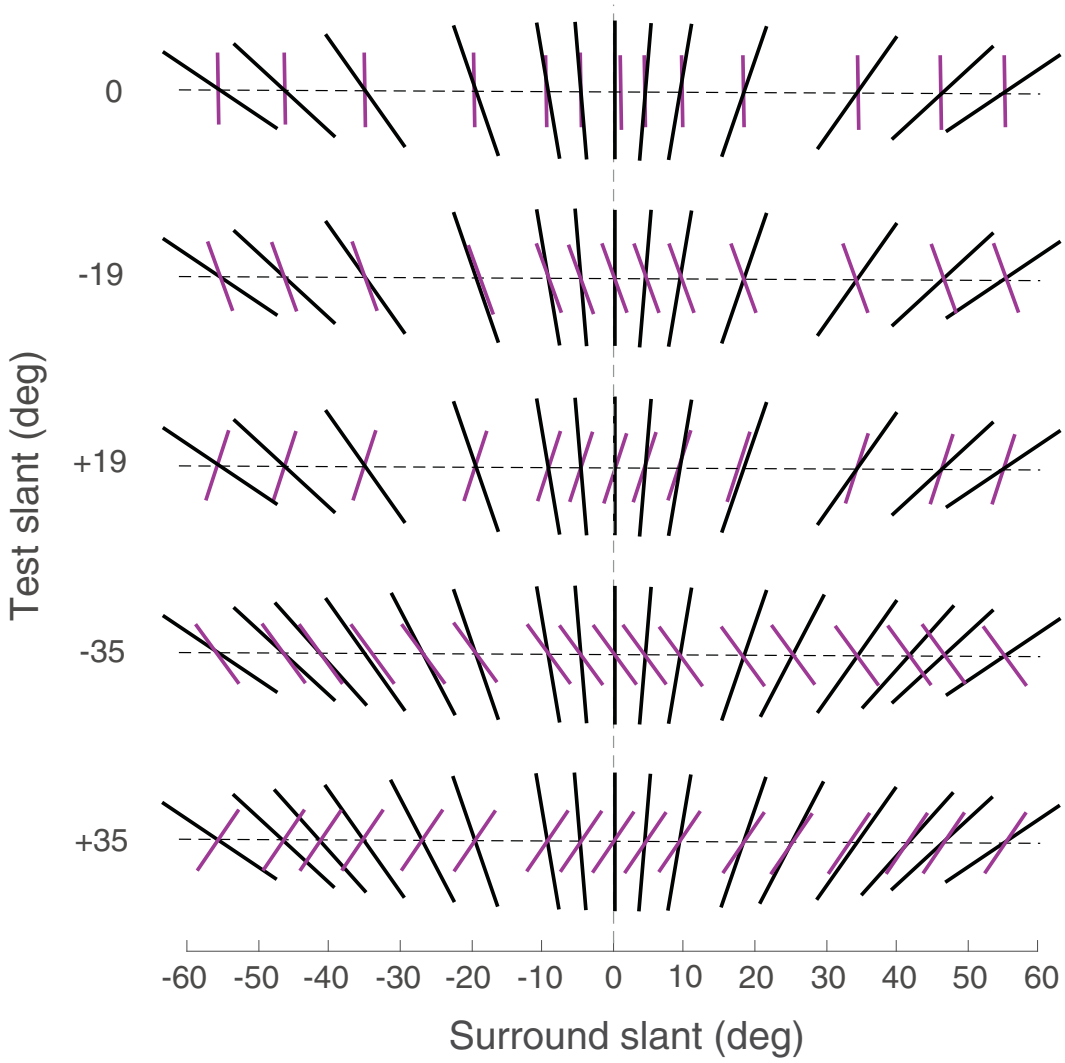

Figure 2. Stereo slant conditions. Black lines represent surrounds; magenta lines, tests. Test slants vary along the ordinate, increasing in absolute magnitude from the top to bottom. Surround slants are shown on the abscissa. When viewed from the left, the lines accurately depict the slant angles employed.

to give a root-mean-square contrast of approximately 0.31.

Because the overlap criterion was determined for the center of each template prior to the allocation of disparity, the LoG micropatterns would in some situations depart somewhat from the 1.25 overlap criterion, which corresponds to a center-to-center LoG separation of 2 *SD*. Because disparity varied only along the vertical axis, the overlap criterion along a given row was always 2 *SD*. However, along the vertical axis, the overlap between neighboring LoGs would on occasion depart from the 2 *SD* criterion. Geometric considerations suggest that the maximum reduction in the overlap would be around 0.02 *SD*, an amount that we assume will have a negligible influence on the results of the study.

The surround and test combinations employed are illustrated in Figure 2. As the figure shows, test slant was fixed for each of the range of surround slants. Each slanted surface was a vertical linear gradient in stereo disparity centered on fixation. Disparity was computed on the basis of orthographic, not perspective, projection. In the stimulus generation software, both test and surround slants were designated by the disparity at the top edge of the surround window, termed the disparity amplitude. Disparity amplitudes were converted to slant angles as described in the Appendix.

Procedure

A staircase procedure was employed to measure the perceived slant of both the test and surround as illustrated in Figure 3. On each trial, the match stimulus preceded the test-plus-surround stimulus to minimize

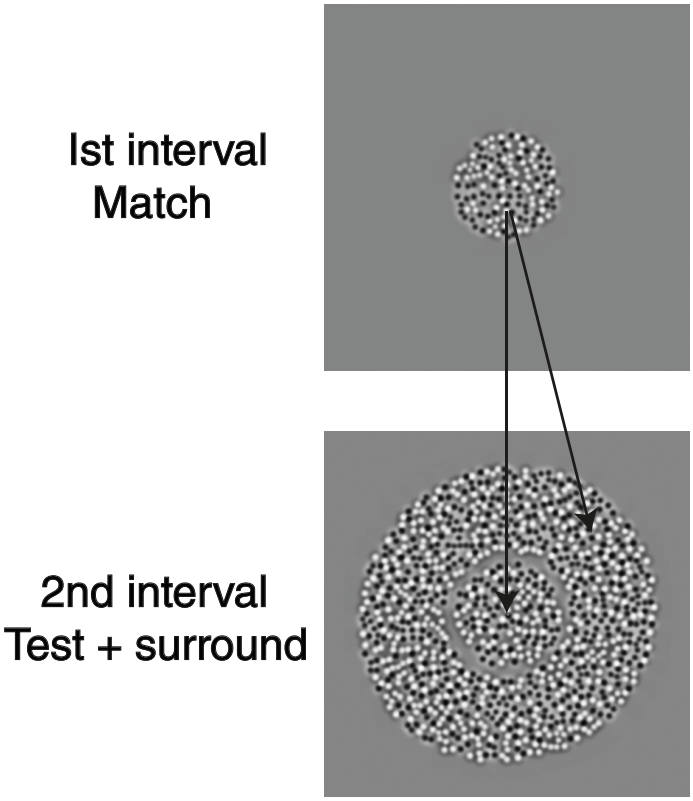

Figure 3. Matching method. Match and test-plus-surround stimuli were presented in temporal order on each trial. The slant of the match stimulus (top) was adjusted using a staircase procedure to match the perceived slant of either the test or surround. See text for further details.

any adaptative effect of the surround on the match stimulus. Each stimulus was presented for 500 ms in a raised cosine temporal envelope to minimize sharp transients, and there was a 250-ms gap between the two stimuli in each trial. Two interleaved one-up/one-down staircases were employed to adjust the slant of the match stimulus. At the start of the session, the disparity amplitude of the match stimulus was randomly selected from a range 0.025° to 0.1° for one staircase and from −0.1° to −0.025° for the other, each value being added to the physical disparity amplitude of the stimulus being matched. On each trial, the observer pressed one of two buttons at the top and bottom of the keypad to indicate whether the top or bottom of the match stimulus had to be "pushed away" to make it appear closer in perceived slant to the stimulus being matched. The staircase adjusted the disparity amplitude by 31% of the slant of the stimulus being matched for the first five trials and 22% thereafter. Trials were self-paced with a 400-ms intertrial interval following each button press. Each session had 50 trials (25 per staircase). Observers completed between one and four sessions per condition.

Analysis

Psychometric functions of proportion of "top-button pressed" responses as a function of match disparity amplitude were fitted with a logistic function using a maximum-likelihood criterion implemented by routines customized from the Palamedes toolbox (Prins & Kingdom, 2018). The point of subjective equality (PSE) was estimated at the 50% level. Standard errors of the PSEs were derived from 400 bootstrap samples. If 1% or less of the samples produced PSE estimates that were outside the range of −90° to +90°, they were discarded from the error estimate. A number of observer 1's psychometric functions did not converge during bootstrapping due to their relatively shallow psychometric function slopes, so for these conditions we took the average of the errors of the data points on either side. The PSEs and standard errors measured in terms of disparity amplitude were then converted to slant angles as described in the Appendix, and these are the measures shown in the graphs.

It might be supposed that our slant-angle PSE estimates are biased, as they are derived from PSE estimates derived from psychometric functions based on disparity amplitude, given that slant angle and disparity amplitude are not quite linearly related, as shown in the Appendix. We checked whether this was the case by measuring psychometric functions based on slant angle and compared the resulting PSE estimates with those based on disparity amplitude. We found that, across a wide range of conditions, the average difference in the PSE estimates from the two methods was around 1.5%, which we assume would have a negligible effect on the pattern of results.

Results

Test matches

Figure 4 shows matches to each test slant for a range of surround slants, for all test–surround combinations and for all four observers (note that observer 4 completed only a subset of the range of conditions). A key feature of the figure is the horizontal gray, blue, and orange lines that represent the matches to the test stimulus when the test and surround slants were equal, the value indicated by the positions of the corresponding vertical lines on the abscissa. Bidirectional slant contrast is evidenced wherever the data on either side of the vertical line falls, respectively, above and below the corresponding horizontal line. This appears to be the case in all conditions, except for the data to the right of the vertical line in observer 2's

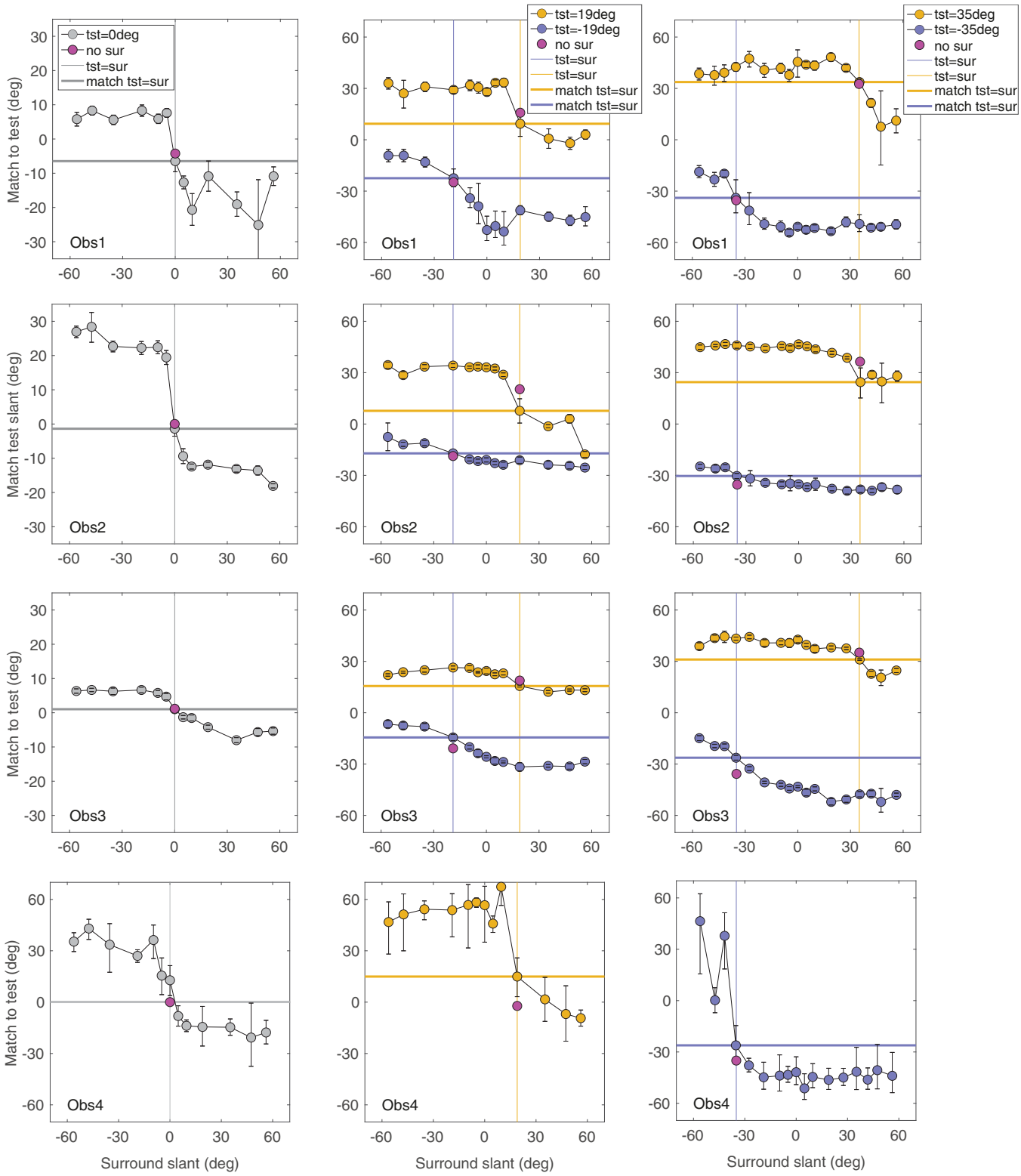

Figure 4. Test matches. Slant angle matches to the central test (tst) pattern are shown as a function of surround (sur) slant angle for four observers (Obs). The panel on the left is for the 0° tests; the middle panel is for the +19° (orange symbols) and –19° (blue symbols) tests; and the panel on the right is for the +35° (orange symbols) and –35° (blue symbols) tests. The true slant of each test is indicated by the position of the vertical lines along the abscissa. Note the different range of match angles for the left panel compared to the middle and right panels. The vertical lines indicate where the test and surround slants are the same and the horizontal lines are the matches for those points. Magenta symbols are matches for the tests in the absence of the surround. Error bars are standard errors derived from bootstrap analysis.

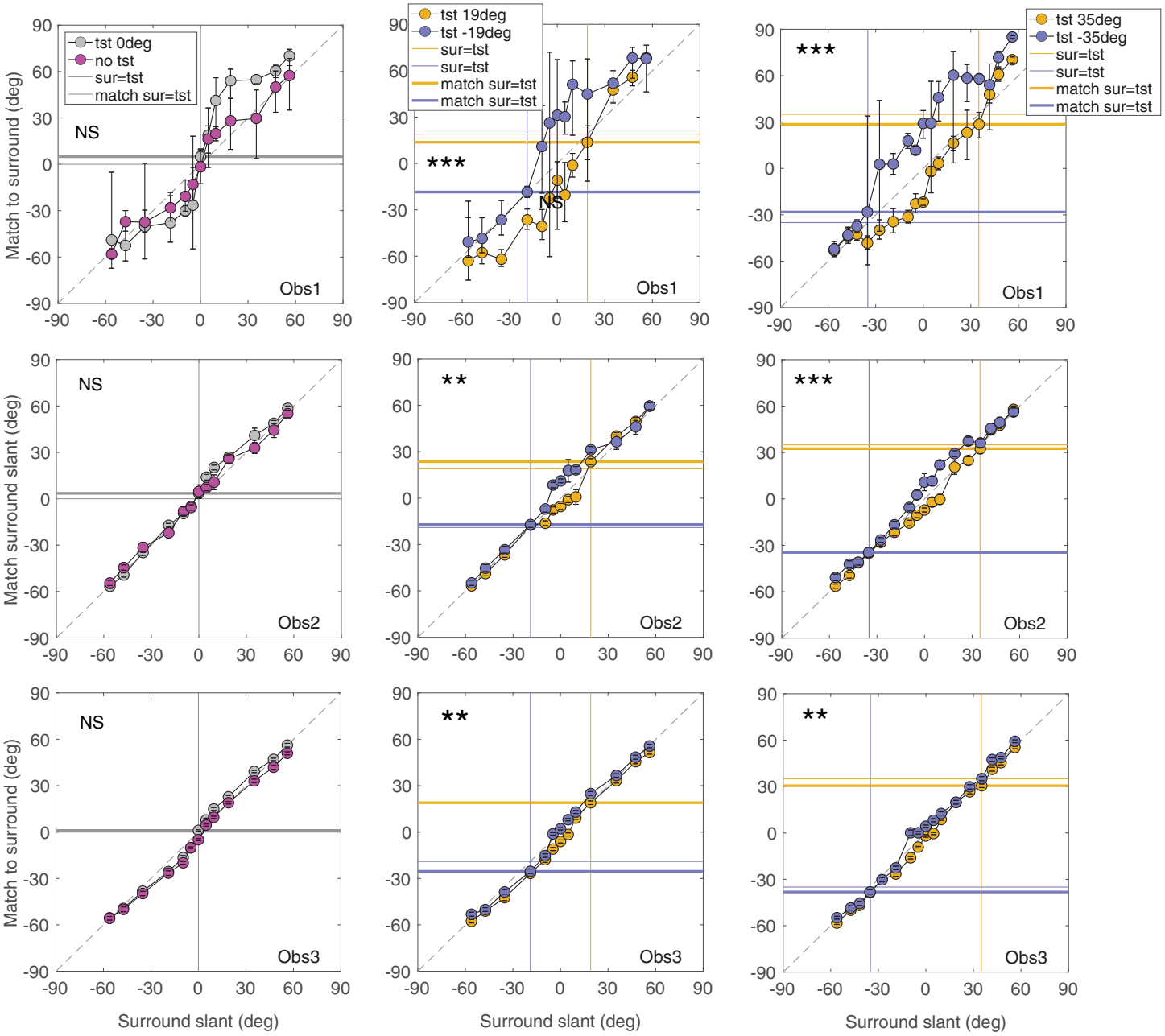

Figure 5. Surround matches. Matches to the slant of the surround are shown as a function of surround angle for both signs of each test slant and for three observers. Symbols and terminology are as for Figure 4, except for the magenta symbols in the panel on the left which show surround matches in the absence of a test. Orange symbols are for positive test slants (+19°, +35°), and blue symbols are for negative test slants (–19°, –35°). The thin vertical and horizontal lines indicate the positions on the two axes of the test slant angles whereas the thick horizontal lines indicate the matches to the surround when test and surround angles are equal. NS, not-significant. Asterisks indicate significance levels for the criterion $p < 0.0056$. See text and Table 1 for details.

+35° test condition. A second feature of the data is that slant contrast appears undiminished when the test and surround slants are in opposite directions, as is evidenced by the fact that there is no obvious difference in the matches on either side of fronto-parallel (0°), the point where the surround switches from one direction to the other. Finally, slant contrast not only is undiminished on either side of fronto-parallel but in most cases remains more or less constant in magnitude as the surround angle approaches its absolute limit. We will return to the significance of these findings in the Discussion.

Surround matches

Does the test induce a contrasting effect on the surround? Figure 5 shows matches to the surround slant

Observer	Test pair	Polynomial	F	df	p	Significance level
1	0, no surround	Quad	1.03	3, 20	0.403	NS
1	0, no surround	Cubic	2.26	4, 18	0.103	NS
1	±19	Quad	27.3	3, 20	< 0.0001	***
1	±35	Quad	25.6	3, 28	< 0.0001	***
2	0, no surround	Quad	2.79	3, 20	0.067	NS
2	0, no surround	Cubic	2.60	4, 18	0.071	NS
2	±19	Quad	9.90	3, 20	0.0003	**
2	±35	Quad	19.5	3, 28	< 0.0001	***
3	0, no surround	Quad	1.97	3, 20	0.152	NS
3	0, no surround	Cubic	3.23	4, 18	0.037	NS
3	± 19	Quad	4.26	3, 20	0.018	NS
3	± 19	Cubic	7.793	4, 18	0.0008	**
3	± 35	Quad	7.95	3, 28	0.0005	**

Table 1. Statistical tests for surround match data, as shown in Figure 5. *F*-tests (*F*), degrees of freedom (df), and *p* values for fitted polynomial parameters to opposite sign test slants. The data were fitted with quadratic (quad) and in some cases also cubic polynomials. The criterion *p* value was Bonferroni corrected to $p < 0.0056$. NS, non-significant. See text for further details.

both with and without the presence of the test. The magenta symbols in the left-hand panel show matches in the absence of the test, and the gray, blue, and orange symbols show matches in the presence of the test. It is clear that the perceived slant of the surround is affected to one degree or another by the presence of the test, as evidenced by the fact that in the left-hand panels the gray and magenta symbols take on a different pattern and in the middle and right-hand panels that the matches to the surrounds with opposite test directions also are also different. There are differences among observers, with a relatively large effect for observer 1 and little effect for the other two observers. Note also that observer 1's error bars are much larger than those of the other two observers and indeed larger than his/her own test match error bars in Figure 4. This is most likely due to observer 1's relatively shallow psychometric function slopes with his/her surround matches.

We conducted statistical tests to determine the significance of the differences between each pairs of curves in Figure 5. For the 0° test, the aim was to determine whether the presence of the test significantly influences the perceived slant of the surround. For the two opposite-in-sign slanted tests, the aim was to compare their differential influence on the perceived slant of the surround, given the additional source of variance the comparison provides. To facilitate a comparison between two sets of data that were clearly not linear, we fitted quadratic and, in some cases, cubic polynomials to each set of data, using Prism (GraphPad, Boston, MA) to test for significant differences between their fitted parameters. Given that there was a total of nine paired comparisons, the criterion level for statistical significance was Bonferroni-adjusted by dividing the standard $p < 0.05$ criterion by 9 to give $p < 0.0056$. The results are shown in Table 1.

For the 0° tests, the quadratic and cubic polynomial fits were not significant. On the other hand, with the slanted tests fitted with quadratic polynomials, all except observer 3's ±19 condition were significant, although when fitted with a cubic polynomial this observer's condition was significant, as indicated in Figure 5 and Table 1.

Is the effect of the test on the perceived slant of the surround a bidirectional contrast effect, as we found for the test matches? To obtain a more direct indication of bidirectionality we first subtracted from the surround matches the match obtained when the test and surround slants were equal, thus normalizing the data to the condition when the test and surround slants formed a planar slanted surface. Second, for the abscissa we subtracted the test slant from all of the surround slants, thus normalizing the abscissa values to zero at the surround-equal-test slant condition.

Figure 6 shows the results. Bidirectionality is evidenced where the points in the lower left quadrant fall below and the points in the upper right quadrant fall above the dashed diagonal line. Observer 1 shows the strongest evidence for bidirectionality, observer 2 less so, and apparently observer 3 barely at all.

To test whether the bidirectionality in the surround match data is significant, we performed an additional normalization in order to reveal the quadrant differences by subtracting from the data the diagonal line values and then separating the data for the lower left and upper right quadrants. For this analysis, the data for the opposite signs of test slant were pooled. Table 2 shows that, in every case, a two-tailed *t*-test revealed significant differences between quadrants at the $p < 0.0056$ criterion, thus confirming that bidirectionality for surround matches was present for both fronto-parallel as well as slanted test conditions.

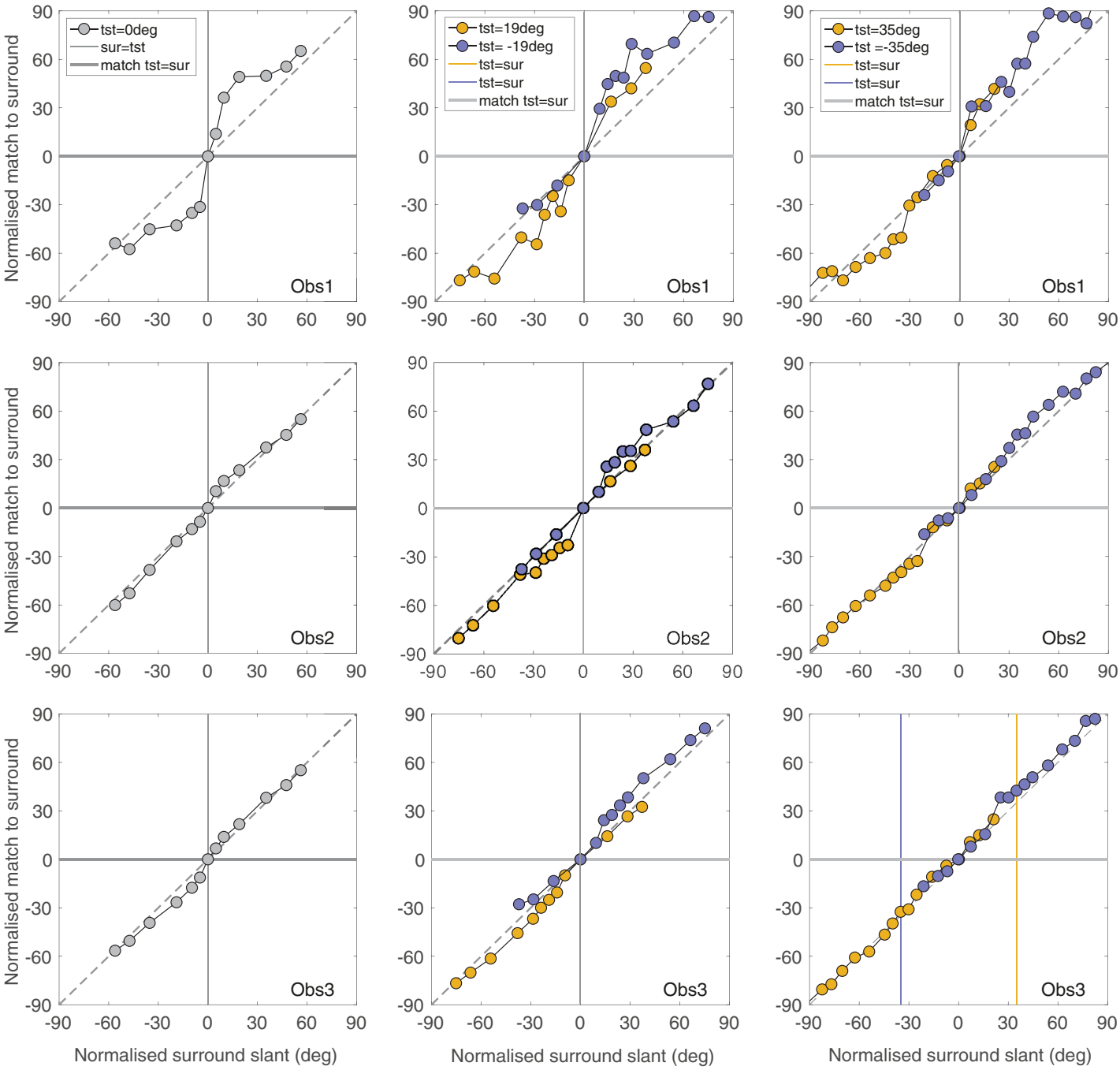

Figure 6. Normalized surround matches. Points in the lower left quadrant that fall below the dashed diagonal line and points in the upper right quadrant that fall above it are indicative of a bidirectional slant contrast effect of the test on the surround. All plots show statistically significant bidirectional effects. See text for further details.

Discussion

Summary of findings

1. We confirmed previous reports that stereo slant contrast is a bidirectional effect, irrespective of whether the central test stimulus is fronto-parallel or slanted (Figures 4 and 6).
2. Stereo slant contrast occurred for opposite as well as same direction of test and surround slant (Figures 4 and 6).
3. Central test slants induced a modest bidirectional contrasting effect on the perceived slant of the

Observer	Test/test pair (deg)	t	df	p	Significance level
1	0	5.17	10	0.0004	**
	±19	8.59	22	<0.0001	***
	±35	8.30	30	<0.0001	***
2	0	3.88	10	0.0031	*
	±19	4.62	22	0.0001	***
	±35	3.65	30	0.001	**
3	0	4.25	10	0.0017	*
	±19	3.47	22	0.002	*
	±35	3.93	30	0.0005	**

Table 2. The t-tests (t) and degrees of freedom (df) for surround matches to 0° test surrounds and slanted test surrounds to test for bidirectionality at the criterion value $p < 0.0056$. See text for further details.

surround, albeit varying in magnitude among the observers (Figure 6).

4. As the test–surround difference increased from zero, slant contrast increased to an asymptotic value and then rarely went into decline (Figure 4).

Comparison with previous findings

In order to compare our results with those of previous findings, we have combined for each observer all matches to the test stimulus into a single plot. Following Figure 3 in van der Kooij and te Pas (2011), which summarizes slant contrast data from several studies, we plotted the data as a function of the difference between surround and test slants. In addition, we normalized each set of data by subtracting from the test matches the match obtained when the test and surround slants were equal. The effect of the two normalizations was to center all of the data around zero in the middle of both axes. We then fitted a sigmoidal, specifically logistic function through the data for each observer to facilitate a direct comparison with the data in van der Kooij and te Pas (2011).

The results are shown in Figure 7 along with the fitted curves in magenta. The plots reveal significant differences between the different test slant conditions both within and between the different observers. Nevertheless bidirectionality is evident throughout, with the exception of observer 2's +35° test condition. Although it is known that stereoacuity varies considerably across the population, both healthy and otherwise (Tittes et al., 2019), there is as far as we know no comparable data for the suprathreshold appearance of stereo-defined surfaces, so without such data it is not possible to tell whether the observer differences in our data are exceptional.

Due to the the effect of averaging the within-subject variations in slant contrast, the fitted curves in Figure 7 fail to adequately capture the steepness of each dataset around the midpoint, nor the asymptotic behavior on either side. Nevertheless, the fits enable us to compare the average size of slant contrast with the data from Figure 3C in van der Kooij and te Pas (2011). If we take the average of all of the absolute endpoints of the fitted curves, we obtain the value of 25°, which is not far from the 20° value obtained from inspection of Figure 3C in van der Kooij and te Pas (2011). The main difference between ours and the data analyzed by van der Kooij and te Pas, apart from the differences in stimulus configurations between the two sets of studies, is that out of the seven studies analyzed by van der Kooij and te Pas, only those by van der Koij and te Pas 2009a, b; van der Koij and te Pas 2009b used non–fronto-parallel test slants, whereas in our study four out of the five sets of data did.

For the effect of the center slant induction on the surround, we know of no previous data that have considered this comparison. The size of induction of test on surround is notably smaller than that of surround on test, and we presume this is because of the relative sizes of test and surround, with the magnitude of induction proportional to the inducer-to-test size ratio as pointed out to us by an anonymous reviewer. We now consider the significance of our results in regard to our understanding of the mechanisms of slant contrast.

Transfer of slant contrast across opposite slant directions

The finding that stereo slant contrast transfers across opposite directions of test and surround slant is interesting, given previous findings from adaptation studies. Using sinusoidally modulated stereo gratings, Rogers and Graham (1985) found an absence of transfer of adaptation across opposite phases of stereo modulation. Their finding is in keeping with the idea that crossed and uncrossed disparities are encoded via different channels and/or that the channels for processing modulated surfaces are spatial-phase selective. A given location on two opposite-direction stereo slanted surfaces (e.g., one like / and the other like \ when viewed from the left) will stimulate opposite disparity channels, so the present results might appear inconsistent with those of Rogers and Graham (1985). However, simultaneous and successive depth contrast may involve different mechanisms, as might also be the case for planar versus modulated stereo-depth surfaces. Stereo-slanted planar surfaces are believed to be processed by channels sensitive to disparity gradients (i.e., the first derivative

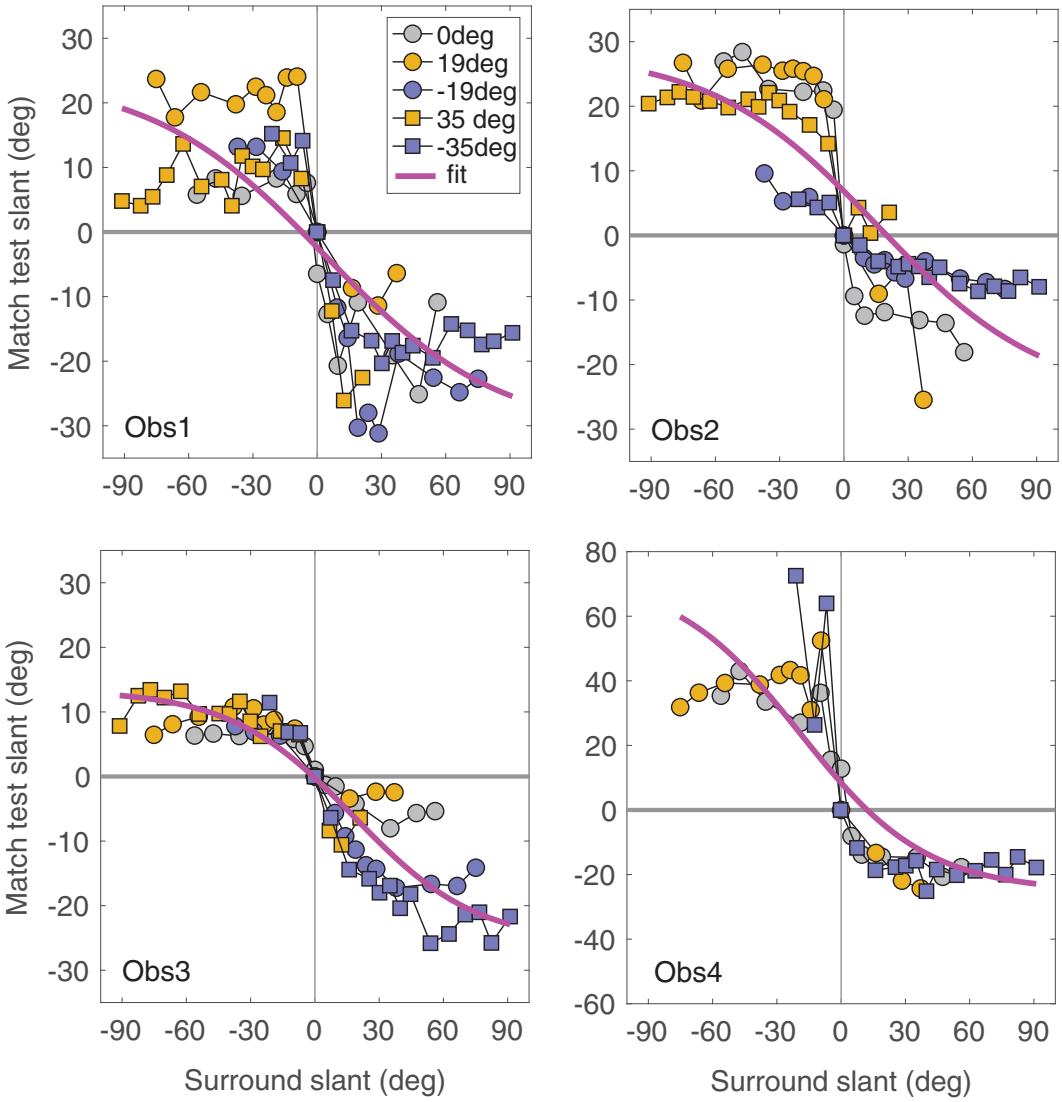

Figure 7. Combined data for each test observer's matches to the central test as a function of surround slant. The data are plotted as a function of the difference between surround and test slant and normalized to the match where test and surround slants are equal. The magenta line is the best-fitting logistic function to each observer's data. Note the expanded range of the *Y*-axis for observer 4. See text for further details.

of disparity) (Bridge & Cumming, 2001; Gillam, Flagg, & Finlay, 1984; Nguyenkim & DeAngelis, 2003; Orban, Janssen, & Vogels, 2006; Parker, 2007; Rogers et al., 1988; Wardle & Gillam, 2016), whereas stereo-modulated surfaces are likely processed by channels sensitive to the second derivative of disparity (Howard & Rogers, 2002). Second-derivative channels are presumably underpinned by neurons whose receptive fields are matched in size to the scale or spatial frequency of the disparity modulation. Future experiments are needed that compare simultaneous and successive contrast using modulated stereo surfaces at different spatial frequencies. It is hoped that such experiments will determine whether or not the transfer of slant contrast across slant direction observed in the present study is unique to planar surfaces or unique to simultaneous as opposed to successive contrast.

Normalization to vertical

The slant of stereo surfaces in laboratory displays is often underestimated, either because of the influence of other cues, in our case for example the absence of perspective (e.g., Sato & Howard, 2001; van Ee et al., 1999), or because of normalization to the vertical (i.e., fronto-parallel plane) (Gilliam, Blackburn, & Brooks, 2007; Gillam, Chambers, & Russo, 1988; Gillam & Pianta, 2005; van de Kooij & te Pas, 2011). The mean

perceived slant of a pair of adjacent slanting surfaces also tends to normalize to the vertical, with their relative slant preserved (Howard & Rogers, 2002; van de Kooij & te Pas, 2011).

Consider in this regard our fronto-parallel test condition. A shift of the mean of test and surround toward vertical while preserving relative slant will shift the test slant away from fronto-parallel in the direction opposite to that of the surround, in keeping with our results as well as those of others. If the test is itself slanted and embedded in a surround with the same direction but lower magnitude of slant, normalization to vertical will again shift the test toward fronto-parallel, as we found. Moreover, there is a hint of normalization to vertical upon examination of the positions of the no-surround data indicated by the isolated magenta symbols in Figure 4. Directly above or below the magenta symbols are the matches made when the test and surround slants are equal, i.e., slanted in the same direction and forming uniformly slanted surfaces. In most cases, the perceived slant of the test is greater when presented alone than when surrounded, an observation that we must thank an anonymous reviewer for pointing out. This is best explained if the effect of the surround is to slightly shift the whole surface towards fronto-parallel, enhancing slant contrast.

The drawback with the normalization-to-vertical account is that if the test and surround are in the same direction but with the test more slanted, there should also be a shift toward vertical (van de Kooij & te Pas, 2011). This would produce a unidirectional, not bidirectional effect of slant contrast, unlike what we found. Therefore, although it is likely that normalization to vertical plays a role in our results, it appears to be insufficient to account for one of its main findings.

Surround inhibition: Analogy with the tilt illusion

Analogous to stereo slant contrast is the well-known tilt illusion, in which an oriented surround pattern (such as a grating) causes a repulsive shift in the perceived orientation of a differently-oriented central test pattern (Akgöz, Gheorghiu, & Kingdom, 2022; Blakemore, Carpenter, & Georgeson, 1970; Clifford, 2014; Schwartz, Sejnowski, & Dayan, 2009). The standard explanation of the tilt illusion is that orientation-selective channels sensitive to the surround inhibit via divisive normalization same-orientation-selective channels sensitive to the test, resulting in a shift in central tendency of the population of channel responses in the test in a direction away from that of the surround. One could account for stereo slant contrast in a similar way by supposing that perceived stereo slant is coded via a population response of channels each selective to a narrow range of slant angles, with channels in the surround inhibiting those of the test. Although the tilt illusion is a potential analog of slant contrast, we suggest caution. The magnitude of the tilt illusion generally peaks at a test–surround difference of around 15°, declines to zero by around 50° to 60°, then, in most situations, reverses in direction before finally returning to zero at 90° (Clifford, 2014). We had anticipated a similar pattern with slant conrast, with a decline to zero at a test–surround slant difference not that far from the peak. However, inspection of the +35° orange and –35° blue symbols in the right-hand panels of Figure 4 shows that even with a test–surround difference of around 90° (the far left point in the orange data and far right point in the blue data), slant contrast for most observers and conditions remained at its asymptotic level. Our attempt at modeling slant contrast using a tilt-illusion-like model has so far failed to predict this result even with channel bandwidth as a variable. Thus, however attractive the tilt illusion is as a potential model for slant contrast, there are important details that remain to be accommodated.

Interactions between disparity-gradient detectors

As discussed earlier, evidence points to stereo slant being encoded by mechanisms sensitive to disparity gradients. Moreover there is additional evidence for mechanisms sensitive to sharp discontinuities between disparity gradients, as occurs at the border between our center and surround surfaces (Deas & Wilcox, 2014; Deas & Wilcox, 2015; Goutcher, Connolly, & Hibbard, 2018; Mamassian & Zannoli, 2020; Wardle & Gillam, 2016). Mechanisms sensitive to disparity-gradient discontinuities could act to enhance slant contrast between center and surround. Moreover, it is possible that the degree of enhancement is invariant to the magnitude of the discontinuity, which would explain the near-asymptotic behavior in slant contrast we observed. Hence, we argue that mechanisms sensitive to disparity surface discontinuities likely play an important role in stereo slant contrast.

Effects of uncertainty

Notable in the surround matches are the large between-observer differences. As Figure 5 shows, the error bars for observer 1 are much larger than those of the other two observers, attributable we argued to the observer's relatively flat psychometric functions in this condition. Also notable is that the magnitude of slant contrast is largest in observer 1's data (see Figure 6). Whatever the cause of observer 1's relatively large

errors, they can be considered as instances of relatively high uncertainty in slant estimation. Bayesian principles have been invoked to explain how relatively high uncertainty can result in greater susceptibility to biases in sensory behavior (Girshick, Landy, & Simoncelli, 2011; van der Kooij & te Pas, 2009a; van der Kooij & te Pas, 2011; Wei & Stocker, 2015; Wei & Stocker, 2017; Weiss, Simoncelli, & Adelson, 2002), consistent with our results. As an anonymous reviewer pointed out, sensory uncertainty may be evident in the combination of smooth within-surface and sharp between-surface disparity gradients, for example a results of reduced reliability in the within-surface mechanism. On the other hand, van der Kooij and te Pas (2011) pointed out that when visual information is impoverished, such as when random perturbations of disparity are added to the surfaces as in the study by van der Kooij and te Pas (2009a), perceptual biases tend to switch from contrast to assimilation. On the basis of the data for observer 1, however, this is the opposite of what we found. It therefore remains unclear as to whether uncertainty mediates the relative magnitude of slant contrast in the present study.

Conclusions

We have measured stereo-slant contrast across a wide range of center and surround slant angles. Of the possible explanations of slant contrast, our results suggest that the interaction between center and surround disparity-gradient detectors is the least problematic and hence our preferred explanation.

Keywords: stereoscopic slant, surround induction, simultaneous contrast, random-dot stereogram, bidirectional contrast

Acknowledgments

The authors especially thank an anonymous reviewer and Can Oluk for invaluable comments and suggestions on an earlier version of the manuscript.

Funded by a grant from the Natural Science and Engineering Council of Canada (MOP 123349 to F.K.) and by summer bursaries from McGill Medical School to Y.Y and C.W.

Commercial relationships: none.
Corresponding author: Frederick A.A. Kingdom.
Email: fred.kingdom@mcgill.ca.
Address: McGill Vision Research, Department of Ophthalmology, Montréal General Hospital, Montréal, QC H3G 1A4, Canada.

References

Akgöz, A., Gheorghiu, E., & Kingdom, F. A. A. (2022). Small angle attraction in the tilt illusion. *Journal of Vision, 22*(8):16, 1–12, https://doi.org/10.1167/jov.22.8.16.

Blakemore, C., Carpenter, R. H. S., & Georgeson, M. A. (1970). Lateral inhibition between orientation detectors in the human visual system. *Nature, 228*(5266), 3739.

Bridge, H., & Cumming, B. G. (2001). Responses of macaque V1 neurons to binocular orientation differences. *Journal of Neuroscience, 21*(18), 7293–7302.

Clifford, C. W. G. (2014). The tilt illusion: Phenomenology and functional implications. *Vision Research, 104*, 3–11.

Deas, L. M., & Wilcox, L. M. (2014). Gestalt grouping via closure degrades suprathreshold depth percepts. *Journal of Vision, 14*(9):14, 1–13, https://doi.org/10.1167/14.9.14.

Deas, L. M., & Wilcox, L. M. (2015). Perceptual grouping via binocular disparity: The impact of stereoscopic good continuation. *Journal of Vision, 15*(11):11, 1–13, https://doi.org/10.1167/15.11.11.

Gillam, B., Blackburn, S., & Brooks, K. (2007). Hinge versus twist: The effects of "reference surfaces" and discontinuities on stereoscopic slant perception. *Perception, 36*, 596–616.

Gillam, B., Chambers, F., & Russo, T. (1988). Postfusional latency in stereoscopic slant perception and the primitives of stereopsis. *Journal of Experimental Psychology, 14*(2), 163–175.

Gillam, B., Flagg, T., & Finlay, D. (1984). Evidence for disparity change as the primary stimulus for stereoscopic processing. *Perception & Psychophysics, 36*(6), 559–564.

Gillam, B., & Pianta, M. J. (2005). The effect of surface placement and surface overlap on stereo slant contrast enhancement. *Vision Research, 45*(25–26), 3083–3095.

Girshick, A. R., Landy, M. S., & Simoncelli, E. P. (2011). Cardinal rules: Visual orientation perception reflects knowledge of environmental statistics. *Nature Neuroscience, 14*(7), 926–932.

Goutcher, R., Connolly, E., & Hibbard, P. B. (2018). Surface continuity and discontinuity bias the perception of stereoscopic depth. *Journal of Vision, 18*(12):13, 1–15, https://doi.org/10.1167/18.12.13.

Goutcher, R., & Wilcox, L. M. (2021). Surface slant impaired disparity discontinuity discrimination. *Vision Research, 180*, 37–50.

Graham, M., & Rogers, B. (1982). Simultaneous and successive contrast effects in the perception of depth from motion-parallax and stereoscopic information. *Perception, 11*(3), 247–262.

Howard, I. P., & Rogers, B. J. (1995). *Binocular vision and stereopsis*. New York: Oxford University Press.

Howard, I. P., & Rogers, B. J. (2002). *Perceiving in depth* (Vol. *2*). New York: Oxford University Press.

Mamassian, P., & Zannoli, M. (2020). Sensory loss due to object formation. *Vision Research, 174*, 22–40.

Nguyenkim, J. D., & DeAngelis, G. C. (2003). Disparity-based coding of three-dimensional surface orientation by macaque middle temporal neurons. *Journal of Neuroscience, 23*(18), 7117–7128.

Oluk, C., Bonnen, K., Burge, J., Cormack, L. K., & Giesler, W. S. (2022). Stereo slant discrimination of planar 3D surfaces: Frontoparallel versus planar matching. *Journal of Vision, 22*(5):, 1–26, https://doi.org/10.1167/jov.22.5.6.

Orban, G. A., Janssen, P., & Vogels, R. (2006). Extracting 3D structure from disparity. *Trends in Neurosciences, 29*(8), 466–473.

Parker, A. J. (2007). Binocular depth perception and the cerebral cortex. *Nature Reviews Neuroscience, 8*(5), 379–391.

Poom, L., Olsson, H., & Börjesson, E. (2007). Dissociations between slant-contrast and reversed slant-contrast. *Vision Research, 47*(6), 746–754.

Prins, N., & Kingdom, F. A. A. (2018). Applying the model-comparison approach to test specific research hypotheses in psychophysical research using the Palamedes toolbox. *Frontiers in Psychology, 9*, 1250.

Rogers, B. J., Cagenello, R., & Rogers, S. (1988). Simultaneous contrast effects in stereoscopic surfaces: The role of tilt slant and surface discontinuities. *Quarterly Journal of Experimental Psychology, 40A*, 417.

Rogers, B. J., & Graham, M. E. (1985). Motion parallax and the perception of three-dimensional surfaces. In D.J. Ingle, M. Jeannerod & D.N. Lee. (Eds.), *Brain mechanisms and spatial vision* (pp. 95–111). Leiden, Netherlands: Martinus Nijhoff.

Sato, M., & Howard, I. P. (2001). Effects of disparity-perspective cue conflict on depth contrast. *Vision Research, 41*(4), 415–426.

Schwartz, O., Sejnowski, T., & Dayan, P. (2009). Perceptual organization in the tilt illusion. *Journal of Vision, 9*(4):19, 1–20, https://doi.org/10.1167/9.4.19.

Tittes, J., Baldwin, A. S., Hess, R. F., Cirina, L, Wenner, Y., & Kuhli-Hattenbach, C., ...Fronius, M. (2019). Assessment of stereovision with digital testing in adults and children with normal and impaired binocularity. *Vision Research, 164*, 69–82.

van der Kooij, K., & te Pas, S. F. (2009a). Uncertainty reveals surround modulation of shape. *Journal of Vision, 9*(3):15, 1–8, https://doi.org/10.1167/9.3.15.

van der Kooij, K., & te Pas, S. F. (2009b). Perception of 3D shape in context: Contrast and assimilation. *Vision Research, 49*(7): 746–751.

van der Kooij, K., & te Pas, S. F. (2011). Perception of 3D slant out of the box. *Frontiers in Psychology, 2*, 119.

van Ee, R., Banks, M. S., & Backus, B. T. (1999). An analysis of binocular slant contrast. *Perception, 28*, 1121–1145.

Wardle, S. G., & Gillam, B. J. (2016). Gradients of relative disparity underlie the perceived slant of stereoscopic surfaces, *Journal of Vision, 16*(5):16, 1–13, https://doi.org/10.1167/16.5.16.

Wei, X.-X., & Stocker, A. A. (2015). A Bayesian observer model constrained by efficient coding can explain 'anti-Bayesian' percepts. *Nature Neuroscience, 18*(10), 1509–1517.

Wei, X.-X., & Stocker, A. A. (2017). Lawful relationship between perceptual bias and discriminability. *Proceedings of the National Academy of Sciences, USA, 114*(38), 10244–10249.

Weiss, Y, Simoncelli, E. P., & Adelson, E. H. (2002). Motion illusions as optimal percepts. *Nature Neuroscience, 5*, 598–604.

Appendix: Calculation of slant angle

Figure A1a depicts a slanted stereo surface viewed from a distance d, with the bottom (or top) of the surface having a disparity η with respect to fixation F. Δd is the distance along the line of sight to the point P with disparity η. According to Howard and Rogers (1995, pp. 36–37), the disparity η at P is given by

$$\eta = \frac{a\Delta d}{d^2 + d\Delta d}$$

where a is the interpupillary distance. Rearranging to give Δd gives

$$\Delta d = \frac{\eta d^2}{a - \eta d}$$

Let the visual angle of the slanted surface in the monocular view be $\alpha°$. Its radius, r, is therefore

$$r = d\ \tan\alpha/2$$

Slant angle θ is therefore

$$\theta = \tan^{-1}\Delta d/r$$

with Δd and r as given above. The approximate interpupillary distances for the three test observers (a) was 7 cm. Viewing distance d was 100 cm, and the visual angle (α) of the stimulus was 8.5°, giving a radius (r) of 7.4 cm. Figure A1b shows the resulting relationship between θ and η.

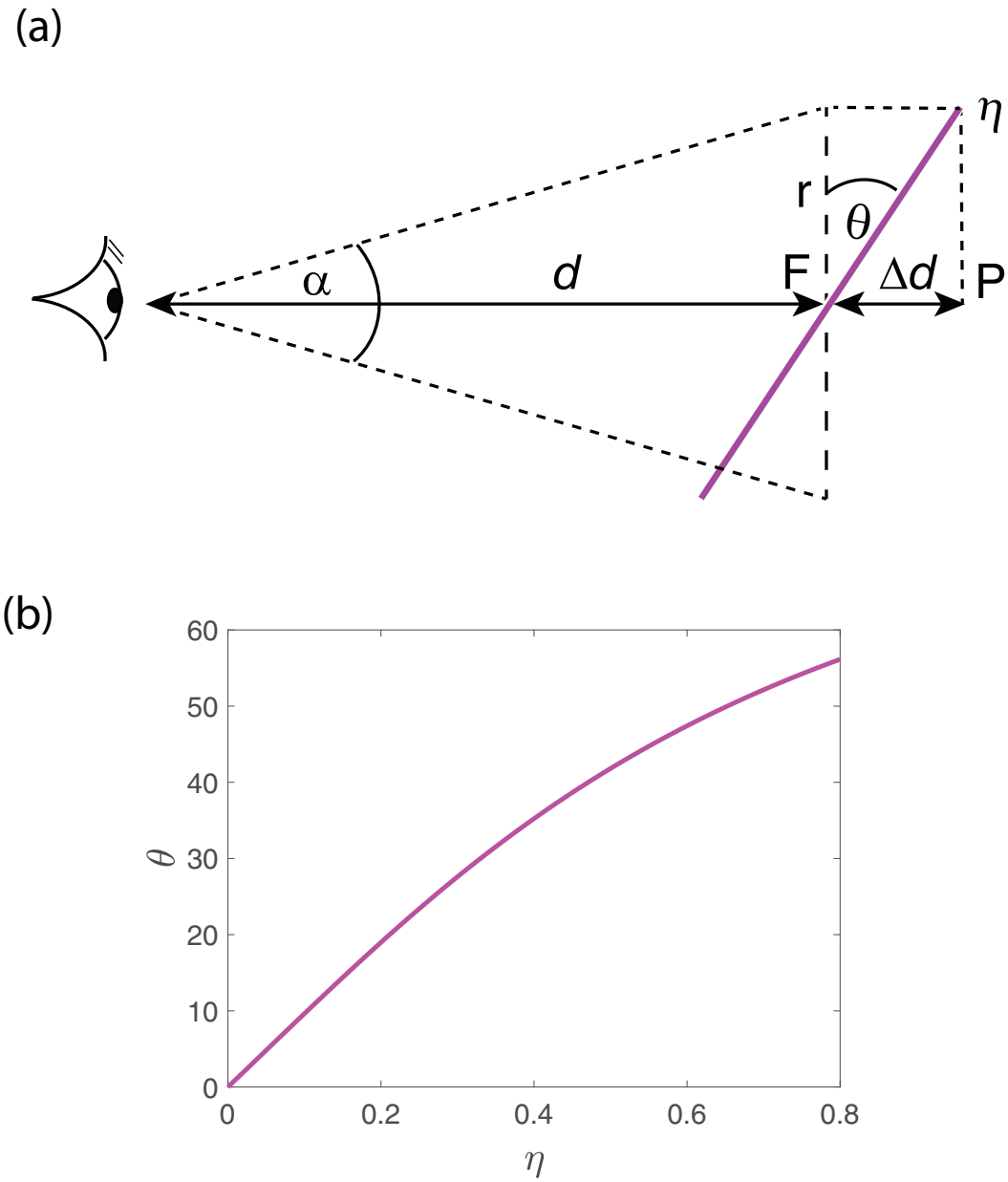

Figure A1. (**a**) Method for converting disparity amplitude η of the slanted surface (purple line) to slant angle θ. See text for details. (**b**) Relationship between θ and η.